
**Separation Science and Technology**
Publication details, including instructions for authors and subscription information:
http://www.informaworld.com/smpp/title~content=t713708471

# Influence of Wall-Retarded Transport on Retention and Plate Height in Field-Flow Fractionation

Joe M. Davis[a]; J. Calvin Giddings[a]
[a] DEPARTMENT OF CHEMISTRY, UNIVERSITY OF UTAH, SALT LAKE CITY, UTAH

**To cite this Article** Davis, Joe M. and Giddings, J. Calvin(1985) 'Influence of Wall-Retarded Transport on Retention and Plate Height in Field-Flow Fractionation', Separation Science and Technology, 20: 9, 699 — 724
**To link to this Article: DOI:** 10.1080/01496398508060700
**URL:** http://dx.doi.org/10.1080/01496398508060700

SEPARATION SCIENCE AND TECHNOLOGY, 20(9 & 10), pp. 699–724, 1985

# Influence of Wall-Retarded Transport on Retention and Plate Height in Field-Flow Fractionation

JOE M. DAVIS and J. CALVIN GIDDINGS

DEPARTMENT OF CHEMISTRY
UNIVERSITY OF UTAH
SALT LAKE CITY, UTAH 84112



**Abstract**

The retarded motion of spherical particles in the vicinity of an FFF channel wall is accounted for in theories for the flow FFF retention ratio and the generalized nonequilibrium plate height. These theories do not quantitatively explain select anomalies reported in the FFF literature.

## INTRODUCTION

Field-flow fractionation is a family of methods especially advantageous for the separation and characterization of macromolecular and colloidal materials. In field-flow fractionation (FFF) each component of a mixture is localized near one wall or boundary of an unpacked channel by a force arising from an external field; components forming zones which are tightly compressed against the wall are carried down the channel by flow more slowly than are the components of less compressed zones, leading to separation. The mechanism of separation has been described more fully in other publications (*1–3*).

The retention of components in FFF is dependent upon the transport rates of the constituent particles. Each particle is subject to two transport processes: one is a field-induced displacement which forces each particle toward the targeted wall (called the accumulation wall), and the other is a diffusive transport process which opposes the buildup of a particle layer at the wall. The steady-state thickness of the particle layer, and thus its




0149-6395/85/2009-0699$3.50/0

retention, is determined by the balance between these two transport processes.

It is well known that the displacement of particles through a viscous medium is inhibited by the presence of other solid objects nearby. A simple case of this is the reduction of particle transport rate when the particle is spherical and is in the proximity of a planar wall. The theoretical details of this wall-retarded transport have been described by Brenner (*4*).

Since sample particles in FFF are forced into a thin layer next to the accumulation wall, each particle will spend a portion of its time in very close proximity to the wall—that is, within a few particle diameters of the wall. In these time intervals, transport rates will be considerably reduced. The question naturally arises as to whether this wall-retarded transport will lead to any serious perturbations in FFF behavior. The present work has been done to determine the magnitude of the wall effect and consequently to provide an answer to the above question.

In the parallel-plate channel configuration used in FFF, illustrated in Fig. 1, the applied field produces a constant or nearly constant force $F$ on the individual particles comprising a component, inducing them to migrate toward the accumulation wall with lateral velocity $U$:

$$U = F/f \tag{1}$$

where $f$, the friction coefficient for the particle, is given by the Planck-Einstein equation as (*5*)

$$f = kT/D \tag{2}$$

where $D$ is the diffusion coefficient of the component particles, $k$ is Boltzmann's constant, and $T$ is absolute temperature.

In the absence of flow, a species composed of infinitesimally small particles forms the following equilibrium concentration profile $c^*(x)$ near the accumulation wall in response to $F$ (*6*):

$$c^*(x) = c_0 e^{-x/l} \tag{3}$$

where $x$ is the distance from the accumulation wall, $c_0$ is the concentration at $x = 0$, and $l$, the characteristic thickness of the profile, is

$$l = D/|U| = kT/|F| \tag{4}$$

where the second equality arises by virtue of Eqs. (1) and (2).

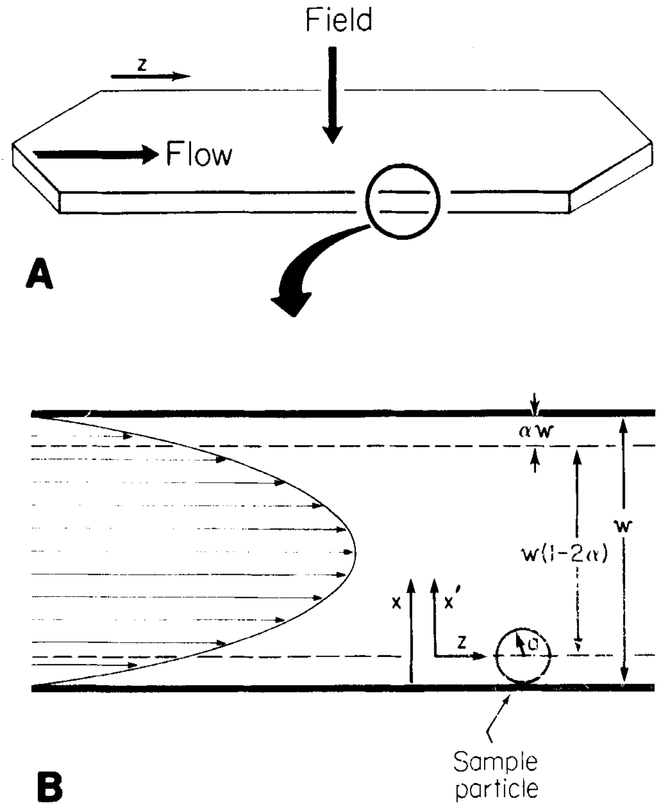


FIG. 1. (A) Schematic of parallel-plate FFF channel. (B) Edge view of channel illustrating coordinate systems.

The flow profile in the FFF channel is closely approximated by the profile of velocity $v$ between infinitely parallel plates:

$$v = 6\langle v\rangle\left(\frac{x}{w} - \left(\frac{x}{w}\right)^2\right) \tag{5}$$

where $\langle v\rangle$ is the average linear velocity of the fluid and $w$ is the width of the channel.

With the help of Eqs. (3), (4), and (5), one can derive the following expression for the retention ratio $R$:

$$R = \text{v}/\langle v\rangle = 6\lambda[\coth(2\lambda)^{-1} - 2\lambda] \tag{6}$$

providing $l$ is constant across the channel. Here $v$ is the average downstream velocity of the component particles and $\lambda = l/w$. Using Eq. (4), we can also write $\lambda$ as $\lambda = kT/|F|w = kT/|W|$, where $W$ is the work done by the constant force $F$ in transporting a particle across the channel of width $w$.

The dispersion of a zone is largely made up of nonequilibrium effects, described by nonequilibrium plate height $H$ (*7*):

$$H = \frac{\chi w^2 \langle v \rangle}{D} \tag{7}$$

where $\chi \equiv \chi(\lambda)$ is a dimensionless nonequilibrium coefficient which approaches $24\lambda^3$ as $\lambda$ approaches zero.

It is usually assumed in the derivation of Eqs. (3), (6), and (7) that transport parameters $D$ and $U$ are constant. We must reconcile this assumption with the knowledge that friction coefficient $f$ increases as a particle approaches within a few equivalent radii of a solid boundary. Thus $D$ and $U$, which vary inversely with $f$ as shown by Eqs. (1) and (2), are not constant over the full width of the channel but decrease very near the walls.

In this paper we account for this wall-retarded transport in the retention and nonequilibrium-plate-height theories of FFF. We wish to determine if reduced transport rates near the walls significantly perturb the equations given above. Since these equations are used to estimate physicochemical properties of resolved species, it is important to know if significant sources of error exist (*6, 8–10*).

Since for most FFF subtechniques, both $D$ and $U$ are inversely proportional to $f$, the ratio $l = D/|U|$ is independent of $f$ and the retention ratio $R$ is thus unaffected by wall-retarded transport. However, for the subtechnique flow FFF, the retention ratio differs from the $R$ expressed by Eq. (6) because Eq. (1) does not describe lateral velocity for this method. A corrected $R$ is obtained later in this paper.

The nonequilibrium plate height is a function of diffusion coefficient $D$, which varies inversely with $f$. Thus a departure from Eq. (7) is expected due to wall-retarded diffusion; its magnitude is also determined in a later section.

## WALL-RETARDED MASS TRANSPORT

The friction coefficient $f$, Eq. (2), is commonly expressed by the Stokes equation (*5*)

$$f_S = 6\pi\eta a \tag{8}$$

where $\eta$ is the viscosity of the fluid and $a$ is the radius of a spherical particle or the effective (Stokes) radius of a nonspherical particle. Equation (8) adequately describes $f$ in bulk fluids but does not account for wall-retarded transport. To describe the latter, we write (*4*)

$$f = \Gamma f_S \tag{9}$$

where $\Gamma$ is a dimensionless term which depends on the shapes of the particle and the wall and the distance between them. The function $\Gamma$, which corrects for the frictional drag on a rigid sphere in the vicinity of an infinite plane, is (*4*)

$$\Gamma = \frac{4}{3} \sinh \gamma \sum_{n=1}^{\infty} \frac{n(n+1)}{(2n-1)(2n+3)} \times \left[ \frac{2 \sinh((2n+1)\gamma) + (2n+1)\sinh 2\gamma}{4 \sinh^2((n+½)\gamma) - (2n+1)^2 \sinh^2 \gamma} - 1 \right], \quad \gamma = \cosh^{-1} \frac{x}{a} \tag{10}$$

where $x$ is the distance of the sphere's center from the plane. A plot of $\Gamma$ versus $x/a$ is shown in Fig. 2; a cursory examination shows that $\Gamma \approx 1$ except within a few radii of the plane. As the sphere approaches the plane (i.e., as $x/a$ approaches 1), $\Gamma$ approaches infinity and mass-transport rates approach zero. Equation (10) has been verified experimentally (*11*).

Also shown in Fig. 2 is a plot of the following approximation to $\Gamma$:

$$\Gamma \approx 1 + \frac{1}{\dfrac{x}{a} - 1} = \frac{x}{x - a}, \qquad x \geqslant a \tag{11}$$

The second term of the middle expression of Eq. (11) can be shown to equal the first-order expansion of Eq. (10) around $x/a = 1$ (*12*). Figure 2 shows that this simple function is a good approximation to $\Gamma$.

We shall use $\Gamma$ to account for the influence of wall-retarded transport on particle behavior in FFF. Such an analysis is rigorous only for spherical particles, but with this case we can gauge the general importance of the wall correction.

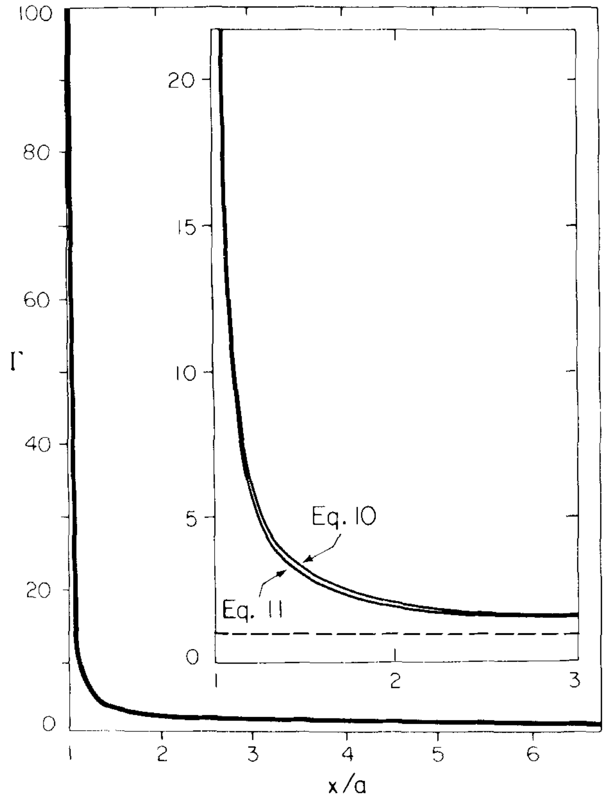


FIG. 2. Plot of Γ, Eq. (10), versus $x/a$. Insert: Plot of Γ and approximation to Γ, Eq. (11), versus $x/a$.



Equation (11) can be written as

$$\Gamma \approx 1 + \frac{a}{x'} \tag{12}$$

where $x' = x - a$ is the distance relative to the plane at $x = a$, as illustrated in Fig. 1(B).

For well-retained components, for which $R \ll 1$, we need to correct for reduced transport rates only at the accumulation wall. Near this wall, Eq. (1) must be modified by Eq. (9) to yield

$$U = \frac{F}{f} = \frac{F}{\Gamma f_s} \tag{13}$$

Similarly, Eq. (2) modified by Eq. (9) gives

$$D = \frac{kT}{f} = \frac{kT}{\Gamma f_S} = \frac{D_S}{\Gamma} \tag{14}$$

where $D_S$ is the Stokes diffusion coefficient applicable to the bulk fluid.

## MODIFIED RETENTION THEORY FOR FLOW FFF

Flow field-flow fractionation is a subtechnique of the FFF family in which components are carried toward the accumulation wall by a lateral flow of fluid through two semipermeable membranes which now constitute the channel walls; the lateral flow displacement replaces the external field (*10, 13–15*). For this method, the lateral velocity $U$ of all particles in the channel is everywhere the same, equaling the transverse flow velocity. The particle diffusion is nevertheless assumed to be retarded in the usual way near the wall of accumulation. Since the ratio $D/U$ of Eq. (4) now depends on $f$ and thus on channel position, the retention ratio $R$, Eq. (6), is no longer rigorously correct for this subtechnique.

We propose here a modified theory of retention for flow FFF in which the magnitude of the lateral velocity is the constant $|U^{\circ}|$ and in which the component's diffusion coefficient is given by Eq. (14). Although the function $\Gamma$ strictly corrects for a particle's decreased diffusivity near a solid plane and not near a semipermeable membrane, this approximation is expected to be fairly good as long as the pore diameter of the membrane (typically about 0.02 μm) is much smaller than particle diameter, which is usually the case.

The retention ratio $R$ for a component subject to any form of FFF, including flow FFF, is given by

$$R = \frac{\langle c^* v \rangle}{\langle c^* \rangle \langle v \rangle} \tag{15}$$

where, as before, $c^*$ is the equilibrium concentration and $v$ and $\langle v \rangle$ are the profile and average linear velocity of the fluid. The angled brackets indicate that the enclosed functions are averaged over the cross section of the channel. The profile of $c^*$ is obtained by equating the net lateral mass flux of the component to zero (*16*):

$$U^\circ c^* - D\frac{dc^*}{dx'} = 0 \tag{16}$$

Using Eq. (14) for $D$, we get

$$\frac{dc^*}{c^*} = \frac{U^\circ \Gamma}{D_S} dx' = -\frac{\Gamma}{l_f} dx' \tag{17}$$

where $l_f \equiv D_S/|U^\circ| = -D_S/U^\circ$ in analogy with Eq. (4). Using Eq. (12) for $\Gamma$ and integrating over the arbitrary $x$ range from $\delta$ to $x'$, we find

$$c^* = c_0 \left(\frac{\delta}{x'}\right)^{a/l_f} e^{-(x'-\delta)/l_f} \tag{18}$$

where $c_0$ is the value of $c^*$ at $x' = \delta$. Equation (18) reduces to Eq. (3) in the limit $a = \delta = 0$, thus satisfying this consistency test.

In terms of coordinate $x'$, the profile of velocity $v$, Eq. (5), is

$$v = 6\langle v\rangle\left(\left(\frac{x'+a}{w}\right) - \left(\frac{x'+a}{w}\right)^2\right) = 6\langle v\rangle\left[(1-2\alpha)\frac{x'}{w} - \left(\frac{x'}{w}\right)^2\right] + 6\langle v\rangle(\alpha - \alpha^2) \tag{19}$$

where $\alpha = a/w$. Combining Eqs. (15), (18), and (19), we find

$$R_f = 6(\alpha - \alpha^2) + \frac{6\int_0^{w(1-2\alpha)}\left(\left(\frac{1-2\alpha}{w}\right)x'^{(1-a/l_f)} e^{-x'/l_f} - \left(\frac{1}{w^2}\right)x'^{(2-a/l_f)} e^{-x'/l_f}\right)dx'}{\int_0^{w(1-2\alpha)} x'^{-a/l_f} e^{-x'/l_f}\, dx'} \tag{20}$$

where $w(1 - 2\alpha)$ is the upper value of the $x'$-coordinate beyond which the spheres' centers cannot migrate (see Fig. 1B). The first term in Eq. (20) is the steric component of retention, originating from the transport of spheres which (almost) touch the wall; these are assumed to be carried at the velocity of the streamline coinciding with the spheres' centers. The second term, the ratio of integrals, describes the Brownian component of retention in the channel's accessible core, which is the fraction of the channel (shown between the dashed lines in Fig. 1B) through which the spheres' centers can move (*17*). This ratio of integrals is zero unless

$0 \leqslant a < l_f$; thus this simple theory for flow FFF predicts that only the steric component of retention exists if $a \geqslant l_f$. For normal FFF, $a < l_f$.

Introducing the variables

$$\zeta_f = x'/l_f \tag{21}$$

and

$$\lambda_f^* = \frac{\lambda_f}{1 - 2\alpha} \tag{22}$$

where $\lambda_f \equiv l_f/w$, we can write Eq. (20) as

$$R_f = 6(\alpha - \alpha^2) + 6\lambda_f \frac{\int_0^{1/\lambda_f^*}((1 - 2\alpha)\, \zeta_f^{(1-a/l_f)} e^{-\zeta_f} - \lambda_f \zeta_f^{(2-a/l_f)} e^{-\zeta_f}) d\zeta_f}{\int_0^{1/\lambda_f^*} \zeta_f^{-a/l_f} e^{-\zeta_f} d\zeta_f}$$

$$= R_s(\alpha) + R_f^*\left(\lambda_f, \frac{a}{l_f}\right) \tag{23}$$

where $R_s$ and $R_f^*$ are, respectively, the steric and accessible-core contributions to retention ratio $R_f$. A similar breakdown of the retention ratio into a steric and a nonsteric term was shown earlier (*17*).

Noting that the integral

$$\int_0^d e^{-m} m^{n-1} dm \equiv P(n,d) \tag{24}$$

is the incomplete gamma function $P(n,d)$, $R_f^*$ may be written as

$$R_f^* = 6\lambda_f \frac{\left((1 - 2\alpha) P\left(2 - \frac{a}{l_f}, \frac{1}{\lambda_f^*}\right) - \lambda_f P\left(3 - \frac{a}{l_f}, \frac{1}{\lambda_f^*}\right)\right)}{P\left(1 - \frac{a}{l_f}, \frac{1}{\lambda_f^*}\right)} \tag{25}$$

If we use the identity

$$P(n,d) = -d^{n-1} e^{-d} + (n - 1) P(n - 1, d) \tag{26}$$

Eq. (25) can be rewritten as

$$R_f^* = 6\lambda_f\left(1 - \frac{a}{l_f}\right)\left[(1 - 2\alpha) - \lambda_f\left(2 - \frac{a}{l_f}\right)\right]$$

$$+ 6\lambda_f \frac{(2\lambda_f - \alpha)\left(\frac{1}{\lambda_f^*}\right)^{(1-a/l_f)} e^{-1/\lambda_f^*}}{P\left(1 - \frac{a}{l_f}, \frac{1}{\lambda_f^*}\right)}, \qquad 0 \leqslant a < l_f \tag{27}$$

As $a$ approaches zero, $R_f^*$ approaches $R$, Eq. (6), thus showing consistency in this limiting case.

The evaluation of the incomplete gamma function $P(1 - a/l_f, 1/\lambda_f^*)$ in Eq. (27) requires either numerical methods or a power-series expansion and subsequent term-by-term integration. For the case in which a component is well retained (i.e., when $\lambda_f \approx \lambda_f^* \ll 1$), the second term on the right-hand side of Eq. (27) is negligible and $R_f^*$ is approximately

$$R_f^* \approx 6\lambda_f\left(1 - \frac{a}{l_f}\right)\left[(1 - 2\alpha) - \lambda_f\left(2 - \frac{a}{l_f}\right)\right], \qquad 0 \leqslant a < l_f \tag{28}$$

The approximate retention ratio $R_f$ for flow FFF which accounts for wall-retarded transport requires that $R_s$ be added to this $R_f^*$, as shown by Eq. (23):

$$R_f \approx 6(\alpha - \alpha^2) + 6\lambda_f\left(1 - \frac{a}{l_f}\right)\left[(1 - 2\alpha) - \lambda_f\left(2 - \frac{a}{l_f}\right)\right],$$
$$0 \leqslant a < l_f \tag{29}$$

A more exact expression for $R_f$ is obtained by adding $R_s$ to the $R_f^*$ of Eq. (27).

## MODIFIED THEORY FOR NONEQUILIBRIUM PLATE HEIGHT

General equations from which the nonequilibrium plate height can be evaluated for species composed of particles of arbitrary shape were derived by Gajdos and Brenner (*18*). In their work the authors noted that a component's diffusion coefficient decreases near the channel wall but did not account for this decrease in their theory. We develop here an equation for the nonequilibrium plate height $H$ of a monodisperse sample composed of spherical particles using the function Γ, the equation of continuity for mass transport, and the nonequilibrium theory of FFF, as developed by Giddings (7). The equation of continuity for mass transport in the channel is (7)

$$\partial c/\partial t = -\nabla \cdot J_l - \nabla \cdot J_z \tag{30}$$

or

$$\frac{\partial c}{\partial t} = -\frac{\partial}{\partial x'}\left(Uc - D\frac{\partial c}{\partial x'}\right) - \frac{\partial}{\partial z}\left(vc - D_z\frac{\partial c}{\partial z}\right) \tag{31}$$

where $t$ is time, $c = c(x',z,t)$ is the component's concentration profile, $J_l$ is the lateral mass flux, $J_z$ is the axial mass flux along coordinate $z$, and $D_z$ is the diffusion coefficient of the species, which is assumed to be constant, relative to flow coordinate $z$.

Nonequilibrium theory is used to calculate $H$ from Eq. (31) as follows. Under quasiequilibrium conditions, profile $c$ does not vary with time along the $x'$-coordinate, and $\partial c/\partial t$ can be approximated as (7)

$$\frac{\partial c}{\partial t} \approx D_z\frac{\partial^2 c^*}{\partial z^2} - \mathrm{v}\frac{\partial c^*}{\partial z} \tag{32}$$

where v is the average zone velocity. Using Eq. (32) and the expansion

$$c = c^*(1 + \varepsilon) \tag{33}$$

where $\varepsilon(x',z)$ is the equilibrium-departure term and measures the fractional departure of $c$ from $c^*$ due to flow (7), an ordinary differential equation in $\varepsilon$ is developed from Eq. (31). It can be further shown that $\varepsilon$ is related to $H = 2\,\mathcal{D}/\mathrm{v}$ by the effective Fickian diffusion coefficient $\mathcal{D}$ measuring flow dispersion (7)

$$\mathcal{D} = -\frac{\langle vc^*\varepsilon\rangle}{\langle c^*\rangle\dfrac{\partial \ln c^*}{\partial z}} \tag{34}$$

where the angular parentheses indicate cross-sectional averages. (All solutions for $\varepsilon$ are proportional to $\partial \ln c^*/\partial z$, so $\mathcal{D}$ is independent of the indicated concentration gradient (7).)

We now derive the differential equation in ε accounting for wall-retarded transport in the channel. Noting that the field-induced velocity $U$ can be written, via Eqs. (3) and (4), as $U = -D/l$ for most FFF subtechniques except flow (which is not considered here), the first term on the right-hand side of Eq. (31) becomes

$$-\nabla \cdot J_l = \frac{dD}{dx'}\left(\frac{c}{l} + \frac{\partial c}{\partial x'}\right) + D\frac{\partial}{\partial x'}\left(\frac{c}{l} + \frac{\partial c}{\partial x'}\right) \tag{35}$$

We may write the partial differential $\partial D/\partial x'$ as $dD/dx'$ since Γ and thus $D$ are functions only of $x'$. Equations (31), (32), (33), and (35) can be combined to give

$$\begin{aligned} D_z\frac{\partial^2 c^*}{\partial z^2} - \mathrm{v}\frac{\partial c^*}{\partial z} = &\frac{dD}{dx'}\left(\frac{c^*}{l} + \frac{c^*\varepsilon}{l} + \frac{\partial c^*}{\partial x'} + \frac{\partial(c^*\varepsilon)}{\partial x'}\right) \\ &+ D\frac{\partial}{\partial x'}\left(\frac{c^*}{l} + \frac{c^*\varepsilon}{l} + \frac{\partial c^*}{\partial x'} + \frac{\partial(c^*\varepsilon)}{\partial x'}\right) \\ &+ D_z\frac{\partial^2 c^*}{\partial z^2} - v\frac{\partial c^*}{\partial z} \end{aligned} \tag{36}$$



where only the indicated terms are kept from the expansion because the zone's axial dimensions are much greater than its lateral dimensions; in other words, because $\partial(c^*\varepsilon)/\partial z \ll \partial(c^*\varepsilon)/\partial x'$ (7). We may consequently write $\partial\varepsilon/\partial x'$ as the ordinary derivative, $d\varepsilon/dx'$.

Equation (36) may be greatly simplified by using the expression

$$\frac{\partial c^*}{\partial x'} = \frac{\partial c^*}{\partial x}\frac{\partial x}{\partial x'} = -\frac{c^*}{l} \tag{37}$$

where $\partial c^*/\partial x'$ is calculated using Eq. (3) and the identity $x = x' + a$.

The substitution of Eq. (37) into Eq. (36), the cancellation of common terms, and regrouping reduces Eq. (36) to

$$(v - \mathrm{v})\frac{\partial c^*}{\partial z} = \frac{dD}{dx'}\frac{d\varepsilon}{dx'}c^* + D\frac{d\varepsilon}{dx'}\frac{\partial c^*}{\partial x'} + D\frac{d^2\varepsilon}{dx'^2}c^* \tag{38}$$

The derivative of $D$ is, using Eq. (14),

$$\frac{dD}{dx'} = -D_S \frac{d\Gamma/dx'}{\Gamma^2} \tag{39}$$

Substitution of Eqs. (37) and (39) simplifies Eq. (38) to the desired differential equation in the equilibrium-departure term ε:

$$\frac{\partial \ln c^*}{\partial z} \frac{\Gamma}{D_S}(v - \nu) = \frac{d^2\varepsilon}{dx'^2} - \left(\frac{d \ln \Gamma}{dx'} + \frac{1}{l}\right) \frac{d\varepsilon}{dx'} \tag{40}$$

If Γ is equated to 1, Eq. (40) reduces to Eq. (20) in Ref. *7*, which is the differential equation in ε for a zone having a constant lateral diffusion coefficient.

Equation (40) may be written in dimensionless form using the reduced variables (*7*)

$$\zeta = x'/l \tag{41}$$

$$\phi = \frac{\varepsilon D_S}{\nu l^2 \dfrac{\partial \ln c^*}{\partial z}} \tag{42}$$

and

$$\mu = v/\nu \tag{43}$$

We then get

$$\frac{d^2\phi}{d\zeta^2} - \left(\frac{d \ln \Gamma}{d\zeta} + 1\right) \frac{d\phi}{d\zeta} = \Gamma(\mu - 1) \tag{44}$$

where $\Gamma(x'/a)$ is transformed to $\Gamma(\zeta)$.

Because the spheres' centers cannot migrate beyond the accessible-core boundaries, it is convenient to calculate first from this differential equation a nonequilibrium plate height $H^*$ for the accessible-core channel (using the approach described above) and then to calculate the measurable nonequilibrium plate height $H$ from $H^*$. Using a formalism previously developed for this purpose (*17*), the constant $6\langle v\rangle(\alpha - \alpha^2)$ is subtracted from $v$, Eq. (19), so that the profile equals zero at the accessible-core boundaries. Parameter $H^*$ can then be shown to equal (*17*)

$$H^* = \frac{\psi^* l^2 \mathrm{v}^*}{D_S} = \frac{x^*(1-2\alpha)^4 w^2 \langle v \rangle}{D_S} \tag{45}$$

where

$$\mathrm{v}^* = R^* \langle v^* \rangle \tag{46}$$

$$v^* = 6\langle v \rangle \left[ (1-2\alpha)\frac{x'}{w} - \left(\frac{x'}{w}\right)^2 \right] \tag{47}$$

$$\chi^* \equiv \psi^* \lambda^{*2} R^* \tag{48}$$

$$\lambda^* = \frac{\lambda}{1-2\alpha} \tag{49}$$

and

$$\psi^* \equiv -2\langle c^* \phi \mu \rangle / \langle c^* \rangle = -2\langle c^*(\phi - g_2)(\mu - 1)\rangle / \langle c^* \rangle \tag{50}$$

where $g_2$ is a constant. The function $v^*$, Eq. (47), is the adjusted velocity profile which equals zero at the accessible-core boundaries. The accessible-core parameters $\mathrm{v}^*$, $\langle v^* \rangle$, and $R^*$ based on this adjusted profile are the average zone velocity, the average linear velocity of the fluid, and the retention ratio, respectively. Parameter $R^*$ is defined by Eq. (6) using $\lambda^*$, Eq. (49), instead of $\lambda$.

The function $\phi$ is obtained by solving Eq. (44) using two constraints to determine a unique solution. The first constraint is that the average departure due to flow of $c$ from $c^*$ is zero (*7*):

$$\langle c^* \varepsilon \rangle = 0 \tag{51}$$

(It is by virtue of this condition that the second identity in Eq. 50 is derived.) The other constraint is that the spheres' centers cannot cross the accessible-core boundaries. Following the method of Giddings, we find (*7*)

$$D\frac{d\phi}{d\zeta} = \frac{1}{\Gamma}\frac{d\phi}{d\zeta}\bigg|_{\substack{\zeta=0 \\ \zeta=1/\lambda^*}} = 0 \tag{52}$$

The function exp $(-\zeta)/\Gamma$ is an integrating factor for Eq. (44); hence

$$\frac{d}{d\zeta}\left(\frac{e^{-\zeta}}{\Gamma}\frac{d\phi}{d\zeta}\right) = e^{-\zeta}(\mu - 1) \tag{53}$$

Integrating both sides, we obtain

$$I = \frac{e^{-\zeta}}{\Gamma}\frac{d\phi}{d\zeta} = \int_0^\zeta e^{-t'}(\mu(t') - 1)dt' \tag{54}$$

where $t'$ is a dummy variable of integration and $I(0) = 0$ in light of Eq. (52). Integrating $I$, we find

$$\phi - g_1 = \int_0^\zeta \Gamma(z')e^{z'} \int_0^{z'} e^{-t'} (\mu(t') - 1)dt'dz' \tag{55}$$

where $z'$ is another dummy variable and $g_1 = \phi(0)$.

Letting the constant $g_2$ in Eq. (50) equal the constant $g_1$ in Eq. (55), we can combine these two equations with Eq. (3) to obtain

$$\psi^* = -2\,\frac{\int_0^{1/\lambda^*} e^{-\zeta}(\mu(\zeta) - 1) \int_0^\zeta \Gamma(z')e^{z'} \int_0^{z'} e^{-t'}(\mu(t') - 1)dt'dz'd\zeta}{\int_0^{1/\lambda^*} e^{-\zeta}d\zeta} \tag{56}$$

The integral in the numerator of Eq. (56) can be simplified via integration by parts, as shown in Ref. *19*. Coefficient $\psi^*$ thus reduces to

$$\psi^* = 2\,\frac{\int_0^{1/\lambda^*} \Gamma e^{\zeta}(\int_0^\zeta e^{-z'}(\mu(z') - 1)dz')^2 d\zeta}{\int_0^{1/\lambda^*} e^{-\zeta}d\zeta} \tag{57}$$

The reduced velocity $\mu = v^*/\text{v}^*$ in the accessible core can be shown, using Eqs. (46) and (47), to equal (*19*)

$$\mu = \frac{6}{R^*}\left(\lambda^*\zeta - (\lambda^*\zeta)^2\right) \tag{58}$$

Combining Eqs. (57) and (58) and partially evaluating the integral, we find

$$\psi^* = \frac{2}{R^{*2}(1 - \exp(-\lambda^{*-1}))} \int_0^{1/\lambda^*} \Gamma e^{\zeta} \left[ 6\lambda^{*2}\zeta^2 e^{-\zeta} + 6(2\lambda^{*2} - \lambda^*)\zeta e^{-\zeta} - \frac{12\lambda^* e^{-\zeta}}{1 - \exp(\lambda^{*-1})} + \frac{12\lambda^*}{1 - \exp(\lambda^{*-1})} \right]^2 d\zeta \tag{59}$$

The complexity of the function Γ, Eq. (10), precludes further analytical evaluation of Eq. (59). We can derive an analytical approximation to $\psi^*$ using the approximation to Γ, Eq. (12), which in terms of ζ is

$$\Gamma \approx 1 + \frac{a}{l\zeta} \tag{60}$$

Combining Eqs. (59) and (60), we obtain an approximation to $\psi^*$ which can be expressed as

$$\psi^*\left(\lambda^*, \frac{a}{l}\right) \approx \psi_i^*(\lambda^*) + \psi_c^*\left(\lambda^*, \frac{a}{l}\right) \tag{61}$$

where $\psi_i^*$ is the nonequilibrium coefficient for an ideal (hypothetical) zone having a constant lateral diffusion coefficient and $\psi_c^*$ is a correction for the restricted motion of zone members near the channel wall. The relationship for $\psi_i^*$ given by Eq. (25) of Ref. *19*, is a complex function of $\lambda^*$ which approaches the limit four as $\lambda^*$ approaches zero. Coefficient $\psi_c^*$ can be shown to equal

$$\psi_c^* = \frac{2a/l}{R^{*2}(1 - \exp(-\lambda^{*-1}))} \left[ 648\lambda^{*4} - 288\lambda^{*3} + 36\lambda^{*2} - (360\lambda^{*3} + 648\lambda^{*4}) \exp(-\lambda^{*-1}) + \frac{72\lambda^*}{1 - \exp(\lambda^{*-1})} \times (6\lambda^{*2}(\exp(-\lambda^{*-1}) - 1) + 6\lambda^* - 1) + \frac{288}{(1 - \exp(\lambda^{*-1}))^2} \times \sum_{n=1}^{\infty} \frac{(\lambda^{*-1})^{2n}}{(2n)(2n)!} \right] \tag{62}$$

Of the six terms in the brackets of Eq. (62), only the first three contribute significantly to the value of $\psi_c^*$ when $R^* \ll 1$. As $\lambda^*$ approaches zero, Eq. (62) approaches $2a/l$; thus the limit of Eq. (61) for this case is

$$\psi^* = 4 + 2\frac{a}{l} \qquad (63)$$

$$\lim \lambda^* \rightarrow 0$$

As $\lambda^*$ and zone thickness $l$ approach zero, Eq. (63) becomes unbounded. Parameter $H^*$ is nevertheless bounded (and approaches zero) because it is proportional to the product $\psi^* l^2$, as shown by Eq. (45).

The function which relates $H^*$ to $H$ is (*17*)

$$H = H^* \frac{R^*(1 - 2\alpha)^2}{6(\alpha - \alpha^2) + R^*(1 - 2\alpha)^2} \qquad (64)$$

Combining Eqs. (45) and (64), we find that

$$H = \frac{\chi^* R^*(1 - 2\alpha)^6 w^2 \langle v \rangle}{D_S[6(\alpha - \alpha^2) + R^*(1 - 2\alpha)^2]} \qquad (65)$$

where $\chi^*$, Eq. (48), is defined by Eqs. (6), (49), and (59) or (61)–(63).



## RESULTS AND DISCUSSION

Figure 3 is a plot of the Brownian (normal or nonsteric) component $R_f^*$ of retention ratio $R_f$ for flow FFF versus $\lambda_f$ for selected values of $a/l_f$. The solid curves were calculated from the rigorous relationship, Eq. (27), with numerical integration of the integral $P(1 - a/l_f, 1/\lambda_f^*)$. The broken curves below the solid ones were calculated from approximate Eq. (28), whereas the broken lines above the solid curves were evaluated from the terms in this expression which are linear in $\lambda_f$. Some approximations are not shown because they essentially superimpose on the solid curves. The agreement between Eqs. (27) and (28) is generally good, especially when the quadratic term in $\lambda_f$ is retained in Eq. (28).

The importance of this modified retention theory for flow FFF is difficult to evaluate. A literature survey reveals that the experimental retention ratios of proteins, polystyrene latices, and viruses in flow FFF systems are in close agreement with the predictions of $R$, Eq. (6), when

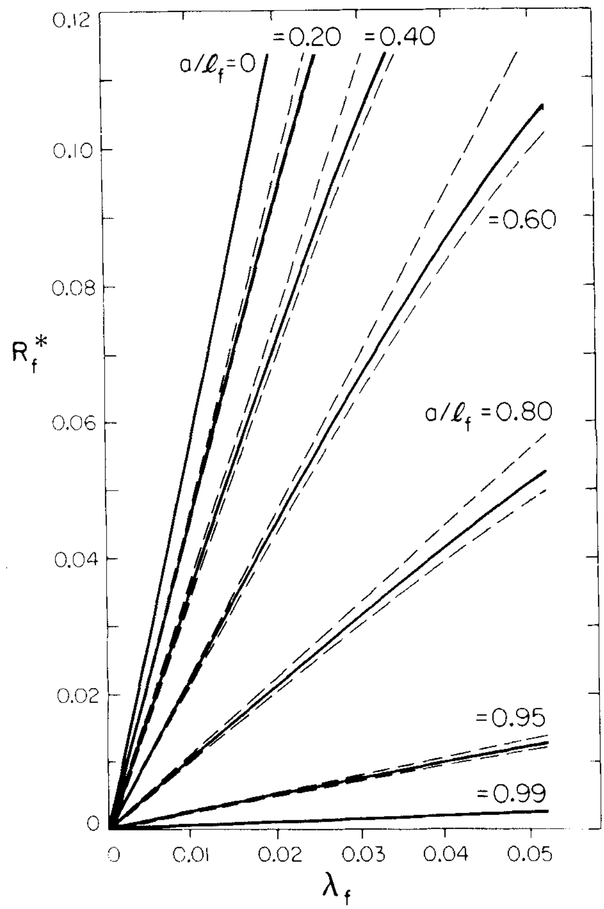


FIG. 3. Plot of $R_f^*$ (for flow FFF) versus $\lambda_f$ for several values of $a/l_f$.

lateral velocity $|U^{\circ}|$ is relatively small (*10, 13, 15*). As observed earlier, however, the retention ratios predicted by Eqs. (6) and (23) are very similar when $a/l_f \ll 1$ and $\alpha \ll 1$.

Using experimental results and physicochemical data characterizing species composed of spherical (or almost spherical) particles, we can estimate $a/l_f$ ratios and determine if a significant departure from Eq. (6) is expected. This ratio can be written, using Eqs. (2) and (8), as (*10*)

$$\frac{a}{l_f} = \frac{a|U^{\circ}|}{D_S} = \frac{a|U^{\circ}|f_S}{kT} = \frac{6\pi\eta a^2 w \dot{V}_c}{kTV_0} \tag{66}$$

where $V_0$ is the column void volume and $\dot{V}_c$ is the volumetric crossflow, the volume of fluid passing through the semipermeable membranes forming the channel walls per unit time. For all but one case, the calculated $a/l_f$ ratios are $\leqslant 0.12$ (and usually $\ll 0.12$). The expected upper percentage error between $R$ and $R_f$ is thus roughly 10%, which is also the average percentage error between Eq. (6) and the experimental retention ratios (*10*). Random sources of error could, however, account for this small relative variation. The exception, a polystyrene latex for which $a/l_f = 0.19$ ($a = 2.4 \times 10^{-7}$ m, $w = 3.8 \times 10^{-4}$ m, $V_0 = 1.85 \times 10^{-6}$ m$^3$, $\dot{V}_c \approx 3.6 \times 10^{-9}$ m$^3$/s, $\eta = 0.001$ kg/m · s, $\lambda_f = 3.33 \times 10^{-3}$, $\alpha = 6.33 \times 10^{-4}$, and $T = 300$ K), is associated with an experimental retention ratio equal to 0.020 (*10*), which is also the retention ratio predicted by both Eqs. (6) and (29). (Although $R_f^*$ is less than $R$, Eq. 6, the flow FFF retention ratio $R_f$ is calculated by adding $R_s$ to $R_f^*$; for this case, $R = R_f$.) Thus none of these results unambiguously establishes the role played by wall-retarded diffusion in the retention mechanism of flow FFF.

Secondly, it has been observed experimentally that some species, e.g., viruses, are infinitely retained in flow FFF systems when lateral velocity $|U^\circ|$ exceeds a critical value (*13*), but complete or partial elution is often observed when $|U^\circ|$ is reduced. The transition is rather sudden. Two possible explanations of this phenomenon are the adsorption of particles on the membrane forming the channel wall and the trapping of particles in microscopic basins of the membrane which are well removed from the axial flowstreams (*13*). Either mechanism could conceivably result in near-infinite retention if particles comprising a zone are very near the membrane, which will be the case when the steric component $R_s$ of retention is the dominant term of retention ratio $R_f$. Equation (23) predicts that only $R_s$ is finite if $a/l_f \geqslant 1$; it is therefore instructive to determine if the critical value of $|U^\circ|$ is obtained when $a/l_f = 1$.

The corresponding critical volumetric crossflow $\dot{V}_{cr}$ is calculated from Eq. (66) by equating $a/l_f$ to unity:

$$\dot{V}_{cr} \stackrel{?}{=} \frac{kTV_0}{6\pi\eta a^2 w} \tag{67}$$

The question mark indicates that Eq. (67) is the expected relationship if the above condition holds. The Qβ virus and similar bacteriophages were reported to adsorb to a cellulose-acetate membrane at the crossflow $\dot{V}_{cr} \approx 1.33 \times 10^{-8}$ m$^3$/s (*13*). Using this value for $\dot{V}_{cr}$ and the values cited above for $V_0$, w, $\eta$, and $T$, the Stokes radius of the Qβ virus calculated from Eq. (67) is 0.284 μm, which is 20.6 times larger than the radius calculated from Eqs. (2) and (8) and the reported Stokes diffusion coefficient of the

Qβ virus, $1.61 \times 10^{-11}$ m$^2$/s (*13*). Since the $a/l_f$ ratio depends on the square of particle radius (see Eq. 66), the actual $a/l_f$ ratio is not unity but $(20.6)^{-2} = 2.36 \times 10^{-3}$, suggesting that little correlation exists between the limit $a/l_f = 1$ and the phenomenon of infinite retention. More likely, an interaction of species with the membrane must be considered to understand this anomaly.

Finally, the apparent decrease in the diffusion coefficient of the Qβ virus with increasing crossflow (*13*) cannot be accounted for by the modified retention theory. For species composed of infinitesimally small particles, λ is (*10*)

$$\lambda = \frac{D_S V_0}{\dot{V}_c w^2} \tag{68}$$



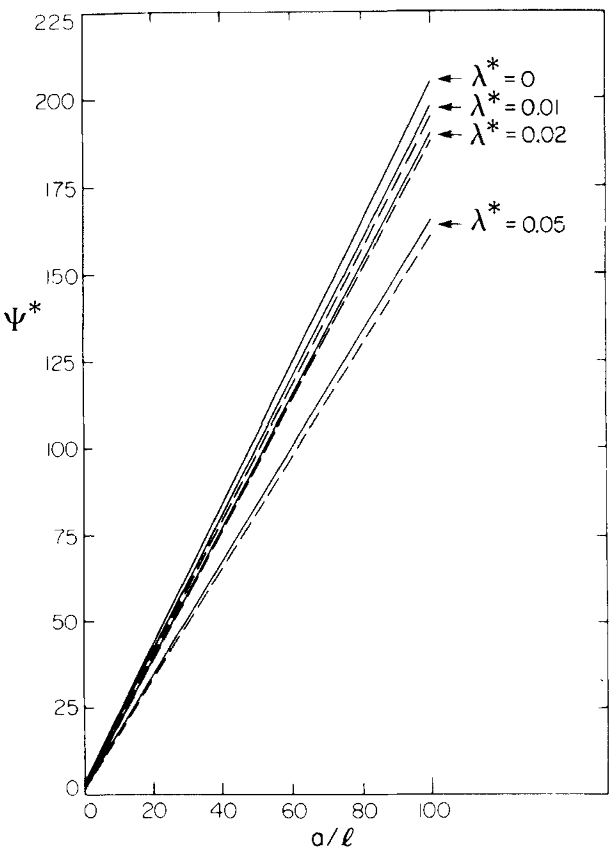


FIG. 4. Plot of ψ* versus $a/l$ for typical values of λ*.

and thus the product $\lambda \dot{V}_c$ is constant and proportional to diffusion coefficient $D_S$. One could propose the following argument to explain the reported decrease in $D_S$. Equation (23) predicts that the expected retention ratio for flow FFF is smaller than predicted by Eq. (6) (assuming $R_f^* \gg R_s$). Using Eq. (6), erroneously small λ's are thus calculated from experimental retention ratios, the relative errors in which increase with increasing crossflow. Thus the product $\dot{V}_c\lambda$ can remain constant only if diffusion coefficient $D_S$ decreases.

Quantitative calculations do not, however, support this argument. In the channel having the cellulose-acetate membrane, the diffusion coefficient of the Qβ virus was reported to decrease when $\dot{V}_c \geqslant 2 \times 10^{-9}$ $m^3/s$ (*13*). Based on this value and the Stokes radius of the virus, the ratio $a/l_f = 3.5 \times 10^{-4}$ is calculated using Eq. (66). Wall-retarded diffusion thus does not account for this phenomenon.

Figure 4 is a plot of the nonequilibrium-plate-height coefficient $\psi^*$ versus $a/l$ for several values of $\lambda^*$. The solid curves were obtained from numerical integration of Eq. (59); the broken curves were evaluated from Eqs. (61) and (62). The limiting curve for $\psi^* = 0$ was calculated from Eq. (63). The agreement between the numerical and analytical results is good.

Figure 5 is a plot of Ξ, the ratio of the nonequilibrium plate height corrected for steric effects (Eq. 64) to the ideal nonequilibrium plate height (Eq. 7), versus $a/l$ for typical values of λ. The solid curves (unlike the broken ones) are also corrected for wall-retarded transport. Clearly, the predicted values of $H$ are greater if one accounts for this effect.

It is premature to evaluate the full significance of this work because, as noted elsewhere (*17*), the importance of size effects on dispersion by f ow has received little experimental study. In general, the agreement betw :en experimental and theoretical nonequilibrium plate heights is not as good as the agreement between experimental and theoretical retention ratios, but this trend is also found in chromatography (*20*).

A brief summary of the discrepancies between experimental and theoretical $H$'s for various FFF subtechniques is helpful in evaluating the importance of wall-retarded transport on nonequilibrium-plate-height theory. In studies of moderately retained ($R \leqslant 0.27$) polystyrene polymers via thermal FFF, excellent agreement between theoretical and experimental χ coefficients was obtained for one series of experiments in two channels (*21*), whereas the percentage error between these coefficients varied from −74.9 to 34.3% for another series of experiments in five channels (*22*). For sedimentation FFF, it was found that plots of $H$ versus $\langle v \rangle$ derived from polystyrene latices (*9*) and the T2 virus (*23*) yielded slopes (which, as shown by Eqs. 7, 48, and 65, are proportional to ψ and

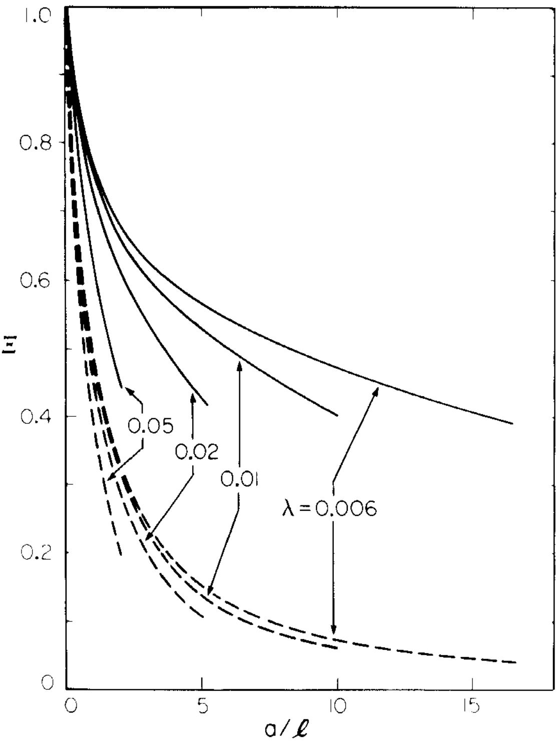


FIG. 5. Plot of dimensionless plate-height ratio, Ξ, versus $a/l$ for typical values of λ. $\alpha \leqslant 0.1$.



$\psi^*$) differing on the average from theory by −42%, most likely due to particle interactions. However, similar studies using polystyrene latices and a different sedimentation system yielded slopes which inexplicably differed from theory by 40–50% (*24*). In a prototypical electrical FFF system with channel walls formed from flexible membranes, the experimental nonequilibrium plate height of hemoglobin was approximately twice the theoretical prediction (*25*), whereas very good agreement between experiment and theory was obtained with the enzyme lysozyme (but not with hemoglobin) in an electrical system with rigid walls (*26*).

The discrepancies between experiment and theory summarized above probably have more than one origin, including system-to-system variation. None of these aberrations, however, is likely attributable to wall-retarded transport. A literature survey reveals that the largest $a/l$ ratio associated with nonequilibrium-plate-height data is 0.38, as determined from the retention of 0.945-μm-diameter polystyrene latex via sedimentation FFF ($w = 1.27 \times 10^{-4}$ m and the retention ratio is 0.08) (*24*). From Eqs. (61), (62), and (65), one anticipates only an 18% variation between the wall-corrected and the ideal nonequilibrium plate heights; furthermore, the theoretical slopes $C$ of the $H$-versus-$\langle v \rangle$ plots for the wall-corrected ($C = 0.61$ s) and the ideal ($C = 0.72$ s) nonequilibrium plate heights are both considerably smaller than the experimental slope ($C = 1.78$ s). This large discrepancy is unlikely due to wall-retarded diffusion.

Most of the experimental studies of plate height summarized above were conducted in the Brownian regime of FFF, for which $l \gg a$. Equation (62) predicts that the corrections to $\psi^*$ and plate height $H$ are most important in the steric regime of FFF, for which $l \ll a$. The experimental data for this regime are unfortunately limited and conflicting (*27–29*). In accordance with nonequilibrium theory, $H$ was found to increase with increasing linear velocity $\langle v \rangle$ for species composed of silica (*27*) and polystyrene latex (*28*) but was found to decrease with increasing $\langle v \rangle$ for a sample composed of red blood cells (*29*).

Furthermore, since for a given field strength radius $a$ almost always is greater for smaller $l$ values (*30*), the $\alpha$ ratios of species readily fractionated via steric FFF are frequently large (i.e., $\alpha > 0.01$). Under these conditions the viscous fluid exerts a nonnegligible lift force on the particles which depends on both $a$ and $\langle v \rangle$ and is opposite to lateral force $F$, inducing migration away from the wall (*28, 29, 31, 32*). Consequently, Eq. (3), which is independent of $a$ and $\langle v \rangle$, is often not correct for the steric mode of FFF, lessening the rigor of coefficient $\psi^*$, Eq. (59). Until further experimental and theoretical characterization of nonequilibrium plate heights in the steric mode of FFF is undertaken, the utility of the wall-corrected equations derived here remains open.



## CONCLUSION

The modified retention theory for flow FFF does not explain quantitatively the infinite retention of a component above a critical crossflow or the apparent decrease in its diffusivity with increasing crossflow. However, the importance of correcting the retention ratio for wall-retarded transport cannot be unambiguously evaluated from published data since usually $a/l_f \leq 0.1$ and the relative errors among $R$, $R_f$, and the experimental retention ratios are all small.

The modified theory for nonequilibrium plate height does not realistically account for several anomalies when components are subject to normal (Brownian) FFF. The influence of wall-retarded diffusion on the nonequilibrium plate heights of components subject to steric FFF cannot be presently evaluated due to insufficient experimental data and an incomplete characterization of the component's concentration profile.

## SYMBOLS

| | |
|---|---|
| $a$ | radius of spherical particle or Stokes radius of nonspherical particle |
| $c$ | concentration |
| $c^*$ | equilibrium concentration |
| $c_0$ | concentration at accumulation wall ($x = 0$) or the plane $x' = \delta$ |
| $D$ | diffusion coefficient |
| $\mathcal{D}$ | effective diffusion coefficient describing flow dispersion |
| $D_S$ | Stokes diffusion coefficient |
| $D_z$ | diffusion coefficient relative to coordinate $z$ |
| $F$ | lateral force on particle subject to FFF |
| $f$ | friction coefficient of particle |
| $f_S$ | Stokes friction coefficient |
| $H$ | nonequilibrium plate height |
| $H^*$ | nonequilibrium plate height in accessible core |
| $J_l$ | lateral mass flux |
| $J_z$ | axial mass flux |
| $k$ | Boltzmann's constant |
| $l$ | $D/\lvert U \rvert$, characteristic thickness of particle layer |
| $l_f$ | $D_S/\lvert U^\circ \rvert$ |
| $P(n,d)$ | incomplete gamma function |
| $R$ | retention ratio |
| $R^*$ | retention ratio in accessible core |
| $R_f$ | retention ratio for flow FFF |
| $R_f^*$ | retention ratio in accessible core for flow FFF |
| $R_s$ | steric component of retention ratio |
| $T$ | absolute temperature |
| $U$ | field-induced lateral particle velocity |
| $U^\circ$ | constant lateral velocity for flow FFF |
| $\dot{V}_c$ | volumetric crossflow |
| $\dot{V}_{cr}$ | critical volumetric crossflow above which infinite retention is observed |
| $v$ | axial velocity of fluid |

| | |
|---|---|
| $v^*$ | adjusted axial velocity of fluid in accessible-core channel |
| $\langle v \rangle$ | average axial velocity of fluid |
| $\langle v^* \rangle$ | average axial velocity of fluid in accessible-core channel |
| $W$ | work required to transport a particle across channel width |
| $w$ | channel thickness or width |
| $x$ | distance from accumulation wall |
| $x'$ | lateral coordinate whose origin is radius $a$ above accumulation wall |
| $z$ | coordinate of flow |
| $\alpha$ | $a/w$ |
| $\Gamma$ | function which corrects for drag on rigid sphere by infinite planar wall |
| $\gamma$ | $\cosh^{-1} x/a$ |
| $\delta$ | lower integration limit for Eq. (17) |
| $\varepsilon$ | equilibrium-departure term |
| $\zeta$ | $x'/l$ |
| $\zeta_f$ | $x'/l_f$ |
| $\eta$ | viscosity |
| $\lambda$ | $kT/\|W\|$ |
| $\lambda^*$ | $\lambda_f/(1 - 2\alpha)$ |
| $\lambda_f$ | $l_f/w$ |
| $\lambda_f^*$ | $\lambda_f/(1 - 2\alpha)$ |
| $\mu$ | reduced velocity |
| $\nu$ | average zone velocity |
| $\nu^*$ | average zone velocity in accessible-core channel |
| $\Xi$ | ratio of steric to ideal nonequilibrium plate height |
| $\phi$ | reduced equilibrium-departure term |
| $\chi$ | nonequilibrium coefficient |
| $\chi^*$ | nonequilibrium coefficient for accessible-core channel |
| $\psi$ | nonequilibrium coefficient |
| $\psi^*$ | nonequilibrium coefficient for accessible-core channel |
| $\psi_c^*$ | correction to coefficient $\psi^*$ due to retarded diffusion at wall |
| $\psi_i^*$ | ideal contribution to coefficient $\psi^*$ |



## Acknowledgments

This work was supported by National Science Foundation Grant CHE-8218503. One of us (J.M.D.) acknowledges fellowship support from the University of Utah Research Committee.

## REFERENCES


1. J. C. Giddings, *Anal. Chem.*, *53*, 1170A (1981).
2. J. C. Giddings, M. N. Myers, and K. D. Caldwell, *Sep. Sci. Technol.*, *16*, 549 (1981).
3. J. C. Giddings, *Ibid.*, *19*, 831 (1984).
4. H. Brenner, *Chem. Eng. Sci.*, *16*, 242 (1961).
5. J. C. Giddings, in *Treatise of Analytical Chemistry: Part I*, 2nd ed., Vol. 5 (I. M. Kolthoff and P. J. Elving, eds.), Wiley, New York, 1982.
6. M. E. Hovingh, G. H. Thompson, and J. C. Giddings, *Anal. Chem.*, *42*, 195 (1970).
7. J. C. Giddings, *J. Chem. Phys.*, *49*, 81 (1968).
8. J. C. Giddings, F. J. F. Yang, and M. N. Myers, *Anal. Chem.*, *46*, 1917 (1974).
9. K. D. Caldwell, L. F. Kesner, M. N. Myers, and J. C. Giddings, *Science*, *176*, 296 (1972).
10. J. C. Giddings, F. J. Yang, and M. N. Myers, *Anal. Chem.*, *48*, 1126 (1976).
11. G. D. M. McKay, M. Suzuki, and S. G. Mason, *J. Colloid Sci.*, *18*, 103 (1963).
12. Unpublished Results.
13. J. C. Giddings, F. J. Yang, and M. N. Myers, *J. Virol.*, *21*, 131 (1977).
14. J. C. Giddings, F. J. Yang, and M. N. Myers, *Science*, *193*, 1244 (1976).
15. J. C. Giddings, F. J. Yang, and M. N. Myers, *Anal. Biochem.*, *81*, 395 (1977).
16. R. B. Bird, W. E. Stewart, and E. N. Lightfoot, *Transport Phenomena*, Wiley, New York, 1960.
17. J. C. Giddings, *Sep. Sci. Technol.*, *13*, 241 (1978).
18. L. J. Gajdos and H. Brenner, *Sep. Sci. Technol.*, *13*, 215 (1978).
19. J. C. Giddings, Y. H. Moon, K. D. Caldwell, M. N. Myers, and M. E. Hovingh, *Sep. Sci.*, *10*, 447 (1975).
20. T. Tsuda and M. Novotny, *Anal. Chem.*, *50*, 632 (1978).
21. L. K. Smith, M. N. Myers, and J. C. Giddings, *Anal. Chem.*, *49*, 1750 (1977).
22. M. Martin, M. N. Myers, and J. C. Giddings, *J. Liq. Chromatogr.*, *2*, 147 (1979).
23. J. C. Giddings, F. J. F. Yang, and M. N. Myers, *Sep. Sci.*, *11*, 553 (1976).
24. J. C. Giddings, G. Karaiskakis, K. D. Caldwell, and M. N. Myers, *J. Colloid Interface Sci.*, *92*, 66 (1983).
25. L. F. Kesner, K. D. Caldwell, M. N. Myers, and J. C. Giddings, *Anal. Chem.*, *48*, 1834 (1976).
26. J. C. Giddings, G. C. Lin, and M. N. Myers, *Sep. Sci.*, *11*, 553 (1976).
27. J. C. Giddings, M. N. Myers, K. D. Caldwell, and J. W. Pav, *J. Chromatogr.*, *185*, 261 (1979).
28. R. E. Peterson II, M. N. Myers, and J. C. Giddings, *Sep. Sci. Technol.*, *19*, 307 (1984).
29. K. D. Caldwell, Z.-Q. Cheng, P. Hradecky, and J. C. Giddings, *Cell Biophys.* *6*, 233 (1984).
30. J. C. Giddings and M. N. Myers, *Sep. Sci. Technol.*, *13*, 637 (1978).
31. K. D. Caldwell, T. T. Nguyen, M. N. Myers, and J. C. Giddings, *Ibid.*, *14*, 935 (1979).
32. P. J. Saffman, *J. Fluid Mech.*, *22*, 385 (1965).


*Received by editor May 1, 1985*